

# Spin Coherence Transfer in Chemical Transformations Monitored by Remote Detection NMR

M. Sabieh Anwar,\* Christian Hilty,† Chester Chu, Louis-S. Bouchard, Kimberly L. Pierce, and Alexander Pines\*

Department of Chemistry, University of California, Berkeley and Division of Materials Science, Lawrence Berkeley National Laboratory, 1 Cyclotron Road, Building 11-D64, Berkeley, California 94720

We demonstrate a nuclear magnetic resonance (NMR) experiment using continuous flow in a microfluidic channel for studying the transfer of spin coherence in non-equilibrium chemical processes. We use the principle of remote detection, which involves spatially separated NMR encoding and detection coils. As an example, we provide the map of chemical shift correlations for the amino acid alanine as it transitions from the zwitterionic to the anionic form. The presented method uniquely allows for tracking the migration of encoded spins during the course of any chemical transformation and can provide useful information about reaction mechanisms.

Analytical chemistry provides us with a mélange of different techniques for monitoring the progress of chemical transformations. A transformation, or reaction, usually manifests itself in a change of some observable property, and the choice of the analytical method depends on the technique's sensitivity, time resolution, and the ability to distinguish between the unmodified and modified states. For example, HPLC has been used to follow the oxidation of glucose;<sup>1</sup> FT-IR has been used for monitoring yields of microwave-assisted fast organic reactions<sup>2</sup> as well as the hydrolysis of monochloroacetate;<sup>3</sup> enzymatic reactions in microreactors have been characterized by fluorescence imaging,<sup>4</sup> and gas chromatography has been employed to determine the progress of Swern oxidations of alcohols.<sup>5</sup>

NMR is also routinely used for monitoring chemical reactions and conformational changes. Recently, NMR has been coupled with microflow systems<sup>6</sup> for studying the kinetics of chemical

reactions,<sup>7</sup> protein unfolding dynamics,<sup>8</sup> and flow profiles.<sup>9</sup> These NMR techniques directly couple to “lab-on-a-chip” devices, multiplexed micro total analysis systems and systems for on-line monitoring of biological and pharmaceutical assays.<sup>10</sup> Some particular advantages of flow-based miniaturized NMR include the following: small volumes of reagents, especially useful when the reagents are expensive or hazardous; increased mass sensitivities;<sup>11</sup> the possibility of hyphenation with complementary spectroscopy and separation techniques;<sup>12</sup> high-throughput, multiplexed detection;<sup>13</sup> and attaining high purities and yields.<sup>14</sup> Specialized microreactors can also be used to enhance the efficiency of mixing, increasing rates of reaction, and optimizing reaction pathways or isolating intermediates by modulation of coil residence times.<sup>5,15</sup>

Most of the previous NMR studies have followed the progress of chemical changes by monitoring the concentrations of molecules as a function of time. This is tantamount to detecting NMR spectra before and after the chemical reaction and monitoring the difference between the two, while time-resolved measurements also enable the monitoring of reaction kinetics. Ciobanu et al. investigated the xylose–borate complexation reaction by measuring the buildup of product peaks over time,<sup>7a</sup> and Wensink et al. monitored the benzaldehyde–aniline reaction by measuring the time-dependent peak areas in the reactant and product spectra.<sup>7b</sup> Recently, the real-time monitoring of fast chemical processes has

\* Corresponding authors. E-mail: sabieh@berkeley.edu; pines@berkeley.edu.

† Now at: Chemistry Department, Texas A&M University, College Station, TX 77843.

- (1) Basheer, C.; Swaminathan, S.; Lee, H. K.; Valiyaveetil, S. *Chem. Commun.* **2005**, 409–410.
- (2) Yoshida, J. *Chem. Commun.* **2005**, 4509–4516.
- (3) Kaun, N.; Kulka, S.; Frank, J.; Schade, U.; Vellekoop, M. J.; Harasek, M.; Lendl, B. *Analyst* **2006**, *131*, 489–494.
- (4) Seong, G. H.; Crooks, R. M. *J. Am. Chem. Soc.* **2002**, *124*, 13360–13361.
- (5) Kawaguchi, T.; Miyata, H.; Ataka, K.; Mae, K.; Yoshida, J. *Angew. Chem., Int. Ed.* **2005**, *44*, 2413–2416.
- (6) (a) Olson, D. L.; Peck, T. L.; Webb, A. G.; Magin, R. L.; Sweedler, J. V. *Science* **1995**, *270*, 1967. (b) Wolters, A. M.; Jayawickrama, D. A.; Sweedler, J. V. *Curr. Opin. Chem. Biol.* **2002**, *6*, 711–716.

- (7) (a) Ciobanu, L.; Tayawickrama, D. A.; Zhang, X.; Webb, A. G.; Sweedler, J. V. *Angew. Chem., Int. Ed.* **2003**, *42*, 4669–4672. (b) Wensink, A.; Benito-Lopez, F.; Hermes, D. C.; Verboom, W.; Gardeniens, H. J. G. E.; Reinhoudt, D. N.; Berg, A. V. D. *Lab Chip* **2005**, *5*, 280–284.
- (8) Kakuta, M.; Jayawickrama, D. A.; Wolters, A. M.; Manz, A.; Sweedler, J. V. *Anal. Chem.* **2002**, *74*, 4191.
- (9) Hilty, C.; McDonnell, E. E.; Granwehr, J.; Pierce, K. L.; Han, S. I.; Pines, A. *Proc. Natl. Acad. Sci. U.S.A.* **2003**, *102*, 14960–14963.
- (10) Clayton, J. *Nat. Methods* **2005**, *2*, 621.
- (11) Seeber, D. A.; Cooper, R. L.; Ciobanu, L.; Pennington, C. H. *Rev. Sci. Instrum.* **2001**, *72*, 2171.
- (12) Jayawickrama, D. A.; Sweedler, J. V. *Anal. Chem.* **2004**, *76*, 4894–4900.
- (13) (a) Raftery, D. *Anal. Bioanal. Chem.* **2004**, *378*, 1403–1404. (b) Hou, T.; Smith, J.; MacNamara, E.; Macnaughtan, M.; Raftery, D. *Anal. Chem.* **2001**, *73*, 2541–2546.
- (14) Watts, P.; Haswell, S. J. *Chem. Soc. Rev.* **2005**, *34*, 235–246.
- (15) (a) Ehrfeld, W.; Hessel, V.; Lowe, H. *Microreactors: New Technology for Modern Chemistry*; Wiley-VCH: New York, 2000. (b) Haswell, S. J.; Middleton, R. J.; O'Sullivan, B.; Skelton, V.; Watts, P.; Styring, P. *Chem. Commun.* **2001**, 391–398.

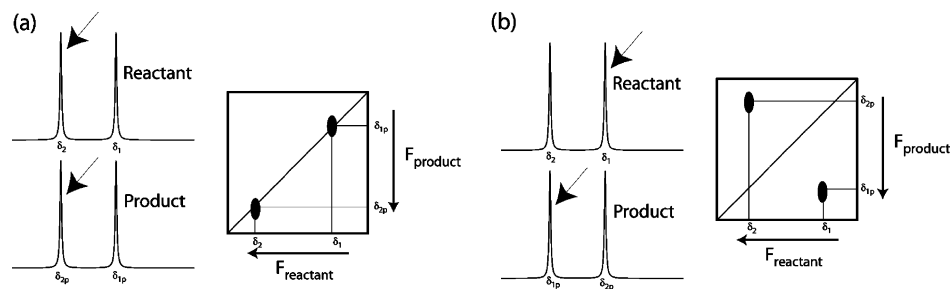


**Figure 1.** Conceptual illustration of the spin coherence transfer, two-dimensional correlation map. (a) The spins do not change their chemical shifts during the transformation from reactant to product and the correlation peaks appear along the diagonal. (b) The spins swap their positions, indicated by the presence of cross-correlated peaks. A conventional “real-time” NMR experiment in the absence of the 2D correlation map cannot distinguish between these two scenarios.

been facilitated by improvements in ultrafast mixing. Some experimental demonstrations have reported mixing times on the order of tens of milliseconds,<sup>16</sup> allowing the study of protein refolding mechanisms in a pH-jump experiment.<sup>17</sup> The method of single-shot multidimensional NMR has also opened up unique possibilities in studying fast chemical reactions,<sup>18</sup> especially when there is a problem of significant peak overlap. In essence, all of these experiments are conceptually similar to taking NMR spectra immediately before and immediately after the sudden change in conditions, such as pH or temperature jumps. At a different level, NMR can also connect between two kinds of molecular conformations existing side by side in a state of dynamic equilibrium. In the reversible transformation  $U \rightarrow V$ , the exchange process can be elucidated by exchange spectroscopy. For example, spin saturation transfer experiments enable one to affect the spectrum of  $U$  by perturbing  $V$ .

The experimental method proposed in this paper is different from the aforementioned experiments because it monitors spin coherence transfers between the reactants and products, rather than measuring only coherence amplitudes. The method can detect not only spectral changes in irreversible, fast chemical transformations of the form  $U \rightarrow V$ , but also correlates spins in the reactant and product species. Suppose, a spin in  $U$  has a chemical shift  $\omega_U$ , and as the same spin migrates to the product  $V$ , it acquires a chemical shift  $\omega_V$ . A conventional real-time experiment will reveal peaks at  $\omega_U$  or  $\omega_V$  or at some intermediate frequency, depending on the kinetics of the reaction. If two spins swap their positions, such as one peak shifting downfield and the other upfield, then unambiguous assignments can become difficult. This ambiguity is exemplified in Figure 1. The proposed method resolves these problems by assigning each spins to a pair  $(\omega_U, \omega_V)$ , corresponding to frequencies before and after the irreversible chemical change, visible as off-diagonal peaks in a two-dimensional NMR experiment. Thus, apart from kinetic data, it can also provide mechanistic information, such as answering the question, where does a particular proton in the product molecule come from in any of the reactants? A thorough understanding of reaction mechanisms is essential for many important chemical and analytical processes. The current study presents an approach for studying

these mechanisms, by tagging spins as they migrate between different chemical species and correlating their initial and final positions.

A forerunner experiment based on a similar idea is the SCOTCH (spin coherence transfer in chemical reactions):<sup>19</sup> a laser-triggered photochemical reaction, correlating the reactant and product spins. This approach is however limited to a class of reactions that are photochemically triggerable. Using our proposed method, the measurement of coherence transfer in any sufficiently rapid reaction that is initiated by the simple mixing of two reactants can be investigated. The detection of a correlation between the chemical shifts of the spins in the reactant and the product is achieved by using two separate coils for encoding and detection of NMR coherence, following the method of remote detection.<sup>20</sup> Previously, this two-coil approach has been used for the independent optimization of the encoding and detection steps, in order to increase NMR sensitivity under certain conditions or for measuring the flow and dispersion properties of a fluid. Tracking spin coherence transfers in chemical processes is a new application of the remote detection methodology.

## EXPERIMENTAL SECTION

Consider the chemical transformation in which  $U$  converts to  $V$  in the presence of  $T$ , which can be either another reactant or a condition inducing the chemical transformation, such as a pH or temperature jump. The nuclear spins in  $U$  change their chemical environment as the chemical transformation takes place. The altered environment results in a change in chemical shift, which can be detected by NMR. If the  $U$  spins have been encoded prior to mixing with  $T$ , it is possible for the two-coil NMR experiment to connect the chemical shifts of the spins in  $V$  with those in  $U$ . This allows us to track the transfer of coherences during the chemical transformation and can be a valuable method for (a) distinguishing between different reaction mechanisms and (b) sensing the presence of the reagent or condition  $T$  and therefore acting as a probe for chemical environments. This experiment is two-dimensional with correlated frequency dimensions, and the results can be presented in the form of a correlation map (discussed below).

(16) Mok, K. H.; Nagashima, T.; Day, I. J.; Jones, J. A.; Jones, C. J. V.; Dobson, C. M.; Hore, P. J. *J. Am. Chem. Soc.* **2003**, *125*, 12484–12492.

(17) Balbach, J.; Forge, V.; van Nuland, N. A. J.; Winder, S. L.; Hore, P. J.; Dobson, C. A. *Nat. Struct. Biol.* **1995**, *2*, 865–870.

(18) Gal, M.; Mishkovsky, M.; Frydman, L. *J. Am. Chem. Soc.* **2006**, *128*, 951–956.

(19) Pouwels, P. J. W.; Kaptein, R. *J. Magn. Reson., Ser. A* **1993**, *101*, 337–341.

(20) (a) Moulé, A. J.; Spence, M. M.; Han, S.-I.; Seeley, J. A.; Pierce, K. L.; Suxena, S.; Pines, A. *Proc. Natl. Acad. Sci. U.S.A.* **2003**, *100*, 9122–9127. (b) Granwehr, J.; Harel, E.; Han, S. I.; Garcia, S.; Pines, A.; Sen, P. N.; Song, Y. *Q. Phys. Rev. Lett.* **2005**, *95*, 075503.

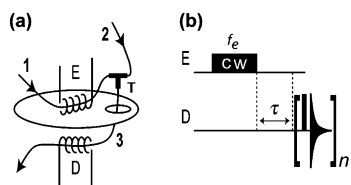


**Figure 2.** (a) Schematics of the experimental NMR setup and (b) pulse sequence used for monitoring the spin coherence transfer. The setup comprises encoding and detection coils E and D, respectively, the inlet capillaries 1 and 2, and the microtee mixer T. In (b), the transmitter frequency in the encoding coil is  $f_e$ ,  $\tau$  is a fixed delay and detection comprises a train of  $n$   $90^\circ$  hard pulses followed by acquisition.

As a model system, we consider a pH-jump experiment: the deprotonation of the amino acid alanine in the presence of a basic medium.<sup>21</sup> At pH = 7.0, the molecule exists as the zwitterion  $\text{NH}_3^+\text{CHCH}_3\text{COO}^-$ , and at basic pH, the amide group is deprotonated resulting in the anion  $\text{NH}_2\text{CHCH}_3\text{COO}^-$ ; the  $\text{pK}_a$  value for the amide proton is 9.7. The increased negative charge on the amide group results in a higher negative charge on the electron-withdrawing groups, increasing the chemical shielding effect and resulting in an upfield shift of the proton resonances. For example, the CH and  $\text{CH}_3$  ( $\alpha$  and  $\beta$ ) protons shift upfield by about 0.6 and 0.4 ppm. With our spatially and temporally separated encoding and detection steps, we map the coherence transfers in the  $\alpha$ - and  $\beta$ -protons as the environment switches from neutral to basic media. For this proof-of-principle experiment, we used 2.0 M alanine in  $\text{D}_2\text{O}$  (pD = 7.0) as the liquid U and 10.0 M NaOD in  $\text{D}_2\text{O}$  (pD = 14.0) as the basic medium T.

Figure 2a shows the schematic setup of the experiment. The liquids U and T are syringe injected into microcapillaries 1 and 2, respectively. The radio frequency (rf) coil E encodes chemical shift information into proton spins in U; the liquids are then allowed to mix in a micro-tee mixer T. Mixing continues as the streams of liquids jointly flow through the outlet capillary 3, where they are finally detected with the rf microcoil D. The encoding and detection is carried out in the homogeneous region of a high field NMR magnet.

The encoded spins travel from coil E to coil D in a certain length of time, called the time of flight  $t_f$ , which depends on the flow rate. Figure 1b shows the NMR pulse sequence for measuring  $t_f$  and also for the remote detection of the magnetization. The sequence comprises a long (500 ms) pulse of low-power continuous wave (CW) irradiation on E. The frequency of the encoding pulse  $f_e$  can be adjusted so that only one narrow spectral region is excited and, in the process, saturated. After a time allowing for physical travel of the encoded species, during which the reaction occurs, the detection is made in D with  $90^\circ$  pulses and acquisition periods of length  $t_{\text{acq}}$ . The pulse–detect combination is repeated  $n$  times, to obtain signal from all encoded spins. Alternatively, it is also possible to use high-power, short-duration  $90^\circ$  pulses for the encoding.<sup>20</sup> However, we encode more spins and obtain higher signal-to-noise ratio by using longer duration low power rf pulses.

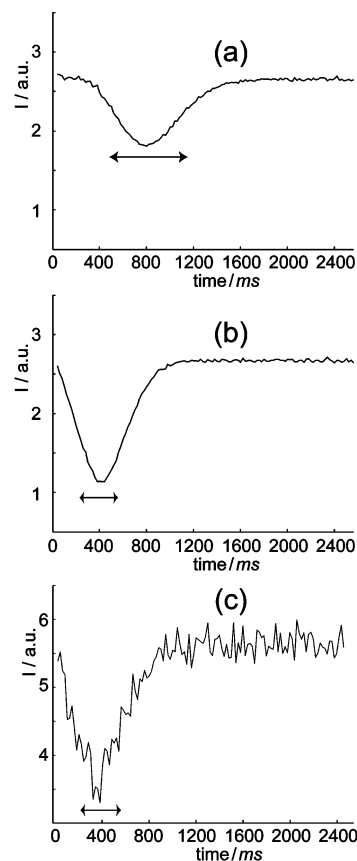


**Figure 3.** Time of travel curves for the  $\text{CH}_3$  peak in ethanol for flow rates of (a) 25 and (b)  $50 \mu\text{L min}^{-1}$  and (c) curve for the  $\beta$ -protons of alanine flowing at  $50 \mu\text{L min}^{-1}$ . The delay  $\tau \approx 0$  ms and  $n = 128$  detection pulses are applied in D with  $t_{\text{acq}} = 20$  ms. The curve in (c) is an average over 32 scans. For the data shown,  $t_f$  is (a) 840, (b) 420, and (c) 380 ms.

The injected spins start off in the equilibrium magnetization  $I_z$ . A  $90^\circ$  pulse in D will convert these spins into observable  $I_x$ , but if the spins have been previously encoded (saturated) in E, the pulse in D leaves them in an unobservable depolarized state. As a result, unencoded spins will produce the maximum intensity in the detection coil spectra, and the intensity will be reduced for the encoded spins. The resulting time of travel curves for two flow rates are shown in Figure 3. The point of minimum intensity in these curves corresponds to the modal time of flight  $t_f$  between the two coils. It can be seen that the breadth of the dip is bigger for the slower flow rate and is indicative of axial dispersion of the fluid as a consequence of laminar flow. The dispersion of the spins compromises the sensitivity of a single acquisition in the detection coil, but can be partially compensated by summing over the FIDs obtained from a selection of points around  $t_f$ . These points are represented by the regions between the arrowheads in the travel curves.

All experiments were performed on a Bruker Avance spectrometer with a proton Larmor frequency of 300 MHz. The PEEK capillaries (Upchurch Scientific) have internal diameters of 100 (1 and 3) and  $150 \mu\text{m}$  (2) and a consistent outer diameter of  $360 \mu\text{m}$ , which fits into the microtee mixer (Upchurch Scientific) with an internal swept volume of  $0.95 \mu\text{L}$ . The fluid was delivered to the NMR magnet through  $1/16$ -in.-o.d. Teflon tubes. The coils E and D are solenoidal microcoils, both of them hand-wound and

(21) (a) Jones, M. *Organic Chemistry*; W.W. Norton & Co., 1997; p 1348. (b) Yarger, J. L.; Nieman, R. A.; Bieber, A. L. *J. Chem. Educ.* **1997**, *74*, 243–246.

each being 3 mm in length. This translates to a detection volume of  $\sim 20$  nL. All chemicals used were obtained from a commercial supplier (Sigma Aldrich). The liquids were injected with a syringe pump (Harvard Apparatus PHD 22/2000 HP), and flow rates typically used varied between 25 and  $100 \mu\text{L min}^{-1}$ . Prior to all experiments, the microcapillaries were purged with acetone and then air to remove any background signal. The  $90^\circ$  high-power pulse widths were 1.1 and  $1 \mu\text{s}$  for the encoding and detection coils. The encoding comprised a long pulse (500 ms) of CW irradiation. The CW encoding power level used was 25 Hz compared to a power of 250 kHz used for the hard pulse. For the remote correlation experiment, the frequency of the encoding pulse was swept over a range of 10.6 ppm in steps of 0.33 ppm.

The two-dimensional experiment that measures the transfer of spin coherence in a chemical process uses the same pulse sequence as given in Figure 2b. The parameters  $\tau$  and  $n$  are selected based on the time of travel curve, so that the acquisition extends over the dip (shown as the regions between the arrowheads in Figure 3). The encoding frequency  $f_e$  is swept across the range of frequencies in the encoding coil, saturating the individual peaks one by one, and if an encoded peak changes its chemical environment during mixing, its chemical shift will appear shifted in the detection coil. It is thus possible to map out correlations between chemical shifts in the encoded and detected dimensions.

## RESULTS

The correlation maps for unmixed ethanol (control experiment) and the zwitterionic and anionic forms of alanine are shown in Figure 4. The two-dimensional data comprise a set of transients, each transient corresponding to one point in the encoding frequency sweep. The intensity from the unencoded spins is removed by subtraction of the respective baseline in each transient. The correlation map shown in Figure 4 is a one-dimensional Fourier transform of the baseline-corrected data. The intensities from the encoding spins will appear as more negative, so that the data are inverted with respect to the baseline and the positive contours are subsequently plotted on a logarithmic scale.

For the ethanol experiment, the spectra do not change across the encoding and detection dimensions as there is no change in chemical environment between E and D, so the alcohol peaks appear in the two-dimensional correlation map along a diagonal, which is shown by the diagonal line in the figure. For the alanine, the  $\alpha$ - and  $\beta$ -protons shift upfield by 0.6 and 0.4 ppm. These shifts are indicated by the presence of off-diagonal peaks in Figure 4b, which clearly indicate the spin coherence transfer during the sudden change in condition, i.e., the introduction of the basic NaOD solution. Note that the frequency axes for the encoding and detection coils are arbitrarily calibrated and appear shifted with respect to each other. This is a result of applying a small magnetic field gradient, provided by the room-temperature  $z$  shim coil of the spectrometer, along the vertical axis to avoid effects from residual cross-talk between the two coils. In the present experiments, the field gradient was set to  $\sim 0.5$  G/cm (corresponding to a frequency difference of 4500 Hz between the two coils separated by nearly 2 cm). In the correlation spectra shown here, it is possible to determine the location of the diagonal from

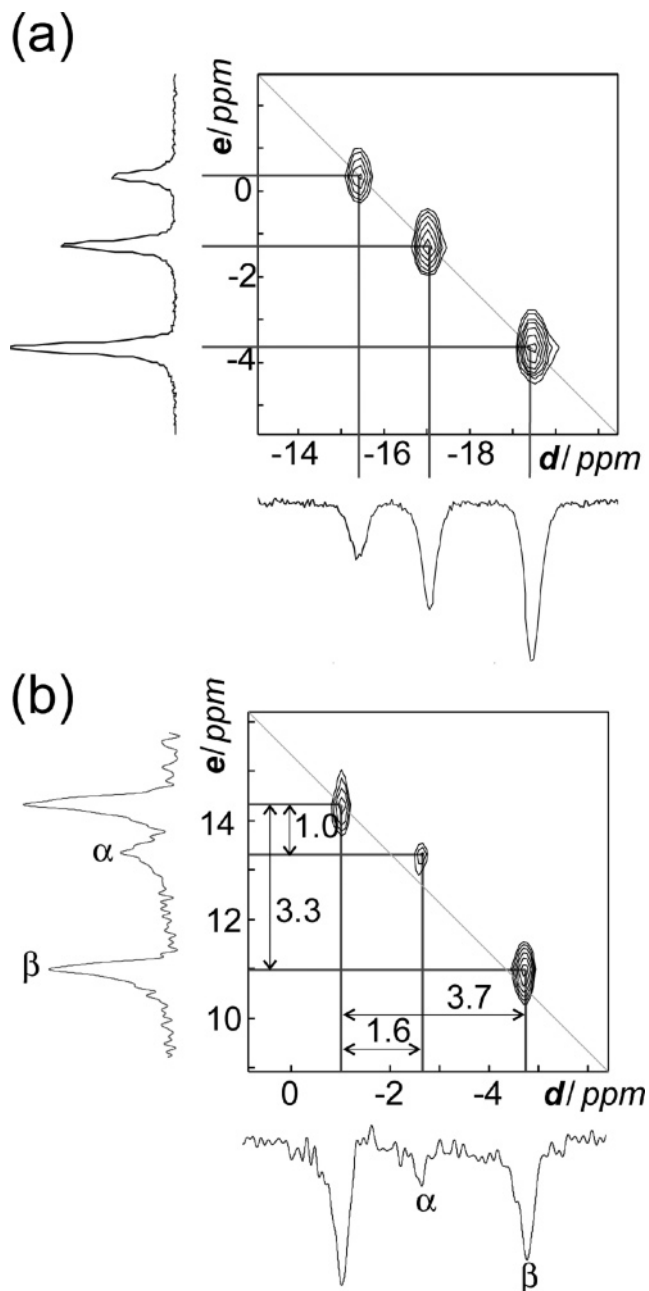


**Figure 4.** (a) Correlation map for the control experiment, ethanol mixed with ethanol, showing only the diagonal peaks, and (b) correlation map between the  $\alpha$ - and  $\beta$ -protons in the zwitterionic and the anionic forms of alanine, showing cross-correlated peaks. The axes  $d$  and  $e$  are chemical shift axes on the detection and encoding coils with units in ppm (uncalibrated). For comparison, the directly detected spectra of the reactant and product, using the respective coils, are superposed on the vertical and horizontal axes respectively. The map in (a) was obtained using a flow rate of  $25 \mu\text{L min}^{-1}$ , and (b) was acquired with a flow rate of  $50 \mu\text{L min}^{-1}$ . Both experiments used an encoding frequency step size of 100 Hz. The unlabeled peak in (b) is assigned to the residual proton signal in the NaOD/D<sub>2</sub>O.

a reactant/product peak that does not change in chemical shift. The chemical shift of water protons is assumed to be independent of pH; this resonance is in fact commonly used as reference for the determination of differences in pH.<sup>22</sup> In general cases, it may be desirable to add a small amount of a reference compound, such as TMS, to the sample for this purpose.

## DISCUSSION AND CONCLUSIONS

The experiment takes advantage of the rapid mixing between the flowing liquids. In the present case, diffusional mixing in a 100- $\mu\text{m}$ -wide channel was used. This mechanism was sufficient for the present application that relied on the exchange of protons, which have a high diffusivity, and will also be adequate for a number of other solutes. In case of reactants with large molecular weight, or solutions of high viscosity, it may be desirable to use more advanced microfluidic mixing technologies.<sup>23</sup> The method presented here is applicable to any chemical transformation that takes place approximately within the spin–lattice relaxation time of the reactants. This relaxation time is on the order of seconds when observing protons, as was the case for the present demonstration experiment. When using carbon-13 spins, the relaxation time is extended to minutes, which should allow exploring a wide range of chemical reactions, including their kinetics. In particular, this method will also be interesting for studying catalyzed reactions, in the homogeneous case where a catalyst is added to one of the liquid streams, or in the heterogeneous case, where a catalyst is immobilized on a matrix inside the channel.<sup>24</sup>

This approach of correlating the premixed and postmixed spectra enables us to directly track the coherence of a spin as it changes its chemical shift due to changes in chemical environment. Chemical changes that can be characterized by the presented method include, but are by no means limited to, the following: changes in the degree of protonation or deprotonation, solvation, complexation,<sup>25</sup> folding and unfolding of proteins,<sup>26</sup> and changes in chemical shift induced by chemical reactions. All of these changes will appear as off-diagonal peaks in the  $e$ – $d$  correlation map, and their presence can be used as a sensitive probe for detecting changes in chemical environments of the spins.

In future experiments, we are considering enhancing the functionality of our experimental setup by increasing the degree of mixing between the incoming liquids using customized “micromixer chips”,<sup>27</sup> improving the spectral resolution by susceptibility matching of the microcoils<sup>28</sup> and the possibility of using stopped-flow, employing a single coil for both encoding and detection. In stopped flow, the fluid U is first injected into the magnet and encoded followed by injection of the fluid T inducing the chemical transformation. In principle, these methods can provide higher spectral resolution as the residence time of the sample inside the sensitive region can be enhanced, enabling longer acquisition times, avoiding the truncation of the FID signal

and also removing the effects of lost signal intensity due to axial dispersion. However, for stopped flow experiments, it is important that the injection time for T is less than the  $T_1$  of the encoded spins in U.

The use of microfluidic mixing has the advantage that it is relatively simple to heat the small fluid volumes to high temperatures if desired, for example, using a small electrical heating element around the capillary. While this was not done in the present work, it would enable studying a wide variety of organic reactions that occur at elevated temperatures. We are also looking into the possibility of investigating more complicated chemical reactions and modifying our pulse sequences for tracking changes in scalar spin–spin couplings, as well as exploring the possibility of accelerated multidimensional experiments.<sup>18</sup> In this context, Fourier encoding by pulsed NMR could be used instead of the selective saturation experiment, similar to present-day multidimensional NMR experiments, and also similar to the original remote detection experiment.<sup>20</sup> This approach presents the advantage of using more elaborate pulse sequences, allowing encoding in multiple frequency dimensions, and corresponding to different nuclei. This may help resolve ambiguities in more complex NMR spectra. As yet another strategy, two-dimensional Hadamard spectroscopy<sup>29</sup> is a promising method allowing the selection of multiple regions in the spectra of the reactant and product molecules. We can envisage excitation of multiple regions in the spectrum using a Hadamard encoded, polychromatic rf pulse, followed by Hadamard decoding in the  $F_1$  and Fourier transformation in the  $t_2$  dimensions. This would also allow faster acquisition and the possibility of targeting only the migrating spin(s). As the Hadamard modulation–demodulation scheme can inherently cancel out certain kinds of systematic errors, one can perform remote detection without the need for phase-cycling protocols generally employed for artifact suppression.

The time-of-flight degree of freedom in the remote detection experiment<sup>20</sup> can be used to provide spatial information about the path through which the various reactants may pass; this can be useful in characterizing complex flow patterns during multiplexed reactions on a chip when the channels have different geometries. Moreover, by varying the mixing time of the experiment, reaction kinetics in longer- $T_1$  species can be followed. Our method also shows promise for detecting multiple parallel or sequential chemical reactions in more complex microfluidic devices in a single experiment. For example, a pulsed-field gradient can be used to spatially encode spectra from different inlet streams, which are later detected after convergence in the detection coil.<sup>27</sup> In this manner, unknown reactants coming from various possible channels can be identified with the incoming channel through the correlation of the spatial encoding and chemical shift dimensions. The resulting data can be seen as containing additional dimensions, one for each phase encoding dimension; an inverse multidimensional Fourier transformation of the hypercomplex data set provides the resolved spatial and chemical correlations. This strategy could, for example, be used to enable multiplexed combinatorial screening of pharmaceutical and biochemical compounds.

(22) Gadian, D. G. *NMR and its applications to living systems*, 2nd ed.; Oxford Science Publishing: New York, 1995.

(23) (a) Yuen, P. K.; Li, G.; Bao, Y.; Müller, U. R. *Lab Chip* **2003**, *3*, 46. (b) Locascio, L. E. *Anal. Bioanal. Chem.* **2004**, *379*, 325–327. (c) Macomber, R. S. *J. Chem. Educ.* **1992**, *69*, 375–378.

(24) Losy, M. W.; Jackman, R. J.; Firebaugh, S. L. *J. Microelectromech. Syst.* **2002**, *11*, 709.

(25) Sijbesma, R. P.; Kentgens, A. P. M.; Nolte, R. J. M. *J. Org. Chem.* **1991**, *56*, 3199–3201.

(26) (a) Shastry, M. C. R.; Roder, H. *Nat. Struct. Biol.* **1998**, *5*, 385–392. (b) Kakuta, M.; Jayawickrama, D. A.; Wolters, A. M.; Manz, A.; Sweedler, J. V. *Anal. Chem.* **2003**, *75*, 956–960.

(27) Harel, E.; Hilty, C.; Koen, K.; McDonnell, E. E.; Pines, A. *Phys. Rev. Lett.* **2007**, *98*, 017601.

(28) (a) Gomez-Hens, A.; Perez-Bendito, D. *Anal. Chim. Acta* **1991**, *242*, 147–177. (b) Olson, D. L.; Lacey, M. E.; Webb, A. G.; Sweedler, J. V. *Anal. Chem.* **1999**, *71*, 3070–3076.

(29) (a) Kupče, E.; Freeman, R. *J. Magn. Reson.* **2002**, *162*, 168–165. (b) Kupče, E.; Nashida, T.; Freeman, R. *Prog. Nucl. Magn. Reson. Spectrosc.* **2003**, *42*, 95–122.

## **ACKNOWLEDGMENT**

This work was supported by the Director, Office of Science, Office of Basic Energy Sciences, Materials Sciences and Engineering Division, of the U.S. Department of Energy under Contract DE-AC03-76SF00098. C.H. acknowledges support from the Sch-

weizerischer Nationalfonds through a postdoctoral fellowship. The authors thank Erin E. McDonnell for hardware assistance.

Received for review December 8, 2006. Accepted January 30, 2007.

AC062327+